A Bioorthogonal Small Molecule Selective Polymeric "Clickase"

Junfeng Chen, Ke Li, Sarah E. Bonson, and Steven C. Zimmerman*

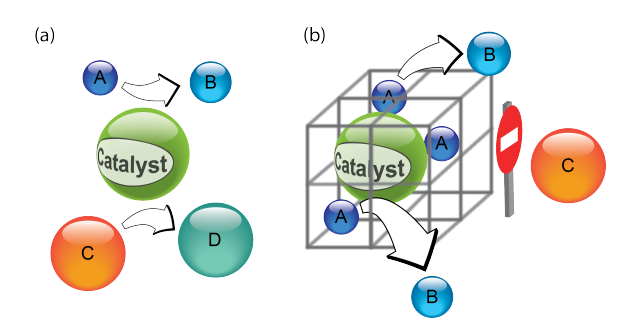
Supporting Information

ABSTRACT: Synthetic polymer scaffolds may serve as gatekeepers preventing the adhesion of biomacromolecules. Herein, we use gating to develop a copper-containing single-chain nanoparticle (SCNP) catalyst as an artificial "clickase" that operates selectively on small molecules that are able to penetrate the polymeric shell. Whereas the analogous clickase with surface ammonium groups performs highly efficient copper(I)-catalyzed alkyne–azide cyclo-addition (CuAAC) reactions on both alkynylated proteins and small molecule substrates, the new SCNP clickase with polyethylene glycol (PEG) groups is only active on small molecules. Further, the new SCNP resists uptake by cells allowing extracellular click chemistry to be performed. We describe two proof of principle applications that illustrate the utility of the bioorthogonal activity. First, the SCNP catalyst is able to screen for ligands that bind proteins, including proteolysis targeting chimera (PROTAC)-like molecules. Second, the non-membrane permeable SCNP can efficiently catalyze the click reaction extracellularly, thereby enabling in situ anticancer drug synthesis and screening without the catalyst perturbing intracellular functions.

INTRODUCTION

Gating has emerged as a useful strategy to control all aspects of chemical catalysis. By caging in a shell (Scheme 1), increased catalyst stability can be achieved and desired substrate selectivity controlled as the surrounding scaffold determines the molecules able to diffuse or bind to the catalytic center. The overall approach has been widely used in multiple areas of chemistry. For example, in supramolecular chemistry, cucurbituril has served as the gate-keeper of a nanoreactor¹ or a metal complex,² in both cases turning on and off catalysis by reversibly blocking access to the active site. Synthetic organic chemists have used metal-organic cages to encapsulate catalysts and alter their stability and accessibility.^{3,4} An example in the biomaterials area involves a PEGylated polymeric micelle that was reported to protect an enzyme from antibody binding and protease degradation, while preserving its activity toward small molecule substrates.⁵

This work is focused on a type of gating by catalytic single-chain nanoparticles (SCNP). Catalytic SCNP have received considerable attention recent years. The polymeric scaffold encapsulates and solubilizes the synthetic catalyst in water, and binds substrates in proximity to the catalytic sites in an enzyme-like manner to achieve high efficiency. Some cationic SCNPs are taken up by cells, retaining their activity and performing intracellular catalysis. Reutral Jeffamine functionalized SCNP catalysts have also shown to



Scheme 1. Schematic illustration of catalyst (a) free in solution and (b) gated by encapsulation.

be able to perform reactions in cells.¹⁹ Previously, we reported the development of a copper containing SCNP as a "clickase." The water-soluble polyacrylamide SCNP1 was covalently cross-linked with BTTAA-like ligands that are particularly effective at stabilizing Cu¹. The artificial clickase performed CuAAC reactions at unprecedented rates by binding small molecule substrates in interior pockets, which was referred to as "uptake mode." Surprisingly we discovered that the same clickase performed highly efficient reactions on protein surfaces. Mechanistic studies showed that the macromolecule to biomacromolecule catalysis was realized through an "attach mode," wherein the SCNP supramolecularly attaches to the protein surface using multivalent interactions.

Given that the CuAAC reaction is one of the most widely used conjugation tools for organic chemistry and chemical biology, ²¹ we sought to expand the utility of Cu¹–SCNP1 as a clickase. In particular, we sought an analogous SCNP that would retain the high CuAAC activity at micromolar concentrations of small molecule substrates in aqueous buffer, ²² but be fully bioorthogonal. Beyond the ability to bind proteins, Cu¹–SCNP1 is taken up by cells through endocytosis, likely because the polycationic SCNP adheres to cell surfaces. Herein, we report Cu¹–SCNP2 with surface PEG groups for water-solubility. This new catalyst performs the bioorthogonal CuAAC click reaction on small molecules with high efficiency, and exhibits its own bioorthogonality. Thus, Cu¹-SCNP2 interacts with proteins weakly and is not taken up by cells, allowing proof of principle experiments such as in situ anticancer drug synthesis and screening for ligand-protein binding.

■ RESULTS AND DISCUSSION

Design and synthesis. SCNP**2** was prepared following our reported "folding and cross-linking" strategy. Thus, poly(pentafluorophenyl acrylate) was post-functionalized with 6-aminohexanoic acid, 3-azidopropylamine, and the mono-MePEG₁₀₀₀ amide of 1,10-decane diamine. The resulting azido polymer was intramolecularly cross-linked with *N,N*-dipropargyl-(1-(*tert*-butyl)-1*H*-1,2,3-triazol-4-yl)methanamine in water using the CuAAC reaction. The resulting covalent cross-linking groups are *N-tert*-butyl-tris(triazolyl)methylamine ligands that, together with the carboxylate groups, act analogously to BTTAA-like ligands.²³

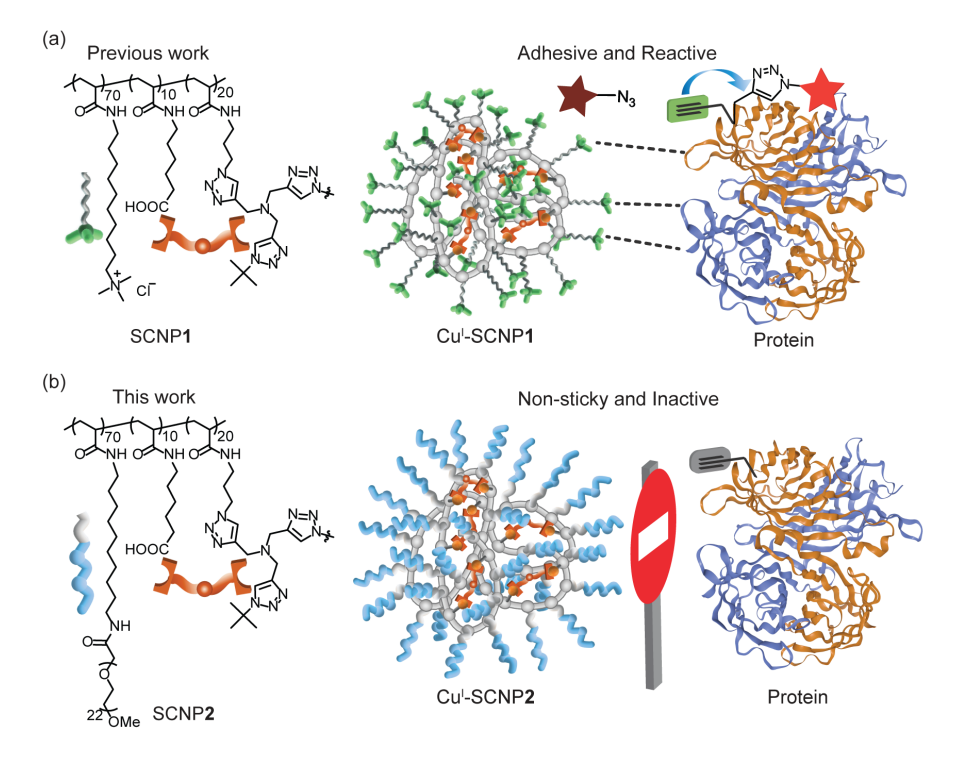


Figure 1. Schematic illustration of the two SCNP catalysts. (a) The structure of cationic SCNP1 which binds and catalyzes reactions on protein surfaces. (b) The structure of PEGylated SCNP2 which does not bind proteins and only perform reactions on small molecules.

The decyl linker units were chosen to provide a hydrophobic binding capacity analogous to that found in SCNP1 whereas the PEG shell conferred water-solubility and resistance to protein and cell binding.

The nanoparticle was purified by dialyzing against water and characterized by dynamic light scattering (DLS, Figure 2a) and transmission electron microscopy (TEM, Figure S1). The diameter of SCNP2 was found to be around 11 nm by DLS, which is higher than that for SCNP1 (6-7 nm) due to its larger molecular weight. After the nanoparticle synthesis and purification, sufficient CuSO₄ was added to give a 1:1 ratio of copper ion to the tris-triazolylmethylamine crosslinks to give Cu^{II}–SCNP2, which can be reduced by sodium ascorbate (NaAsc) to generate the catalytically active Cu^I–SCNP2 in situ.

SCNP-protein binding study. Replacing the cationic trimethylammonium ion groups with PEG groups gives SCNP**2** with a potentially uncharged neutral surface, depending on the location and ionization of the carboxylic acid groups. Indeed, the measured ζ -potential for SCNP**1** and SCNP**2** were 33.9 \pm 1.7 mV and 1.57 \pm 0.64 mV, respectively (Figure 2a), indicating a nearly neutral surface for the latter polymeric nanoparticle. Previously, we reported that the carboxylate groups in SCNP**1** accelerated its click reaction analogous to that found in the small molecule ligand BTTAA.²³ The low ζ -potential for SCNP**2** may indicate that the carboxylic acid groups are protonated, form zwitterionic structures with the tertiary amino groups, or, more likely that the PEG groups provide a neutral surface layer.

To assess its adhesive character, bovine serum albumin (BSA) was chosen as the model protein to measure the potential for SCNP binding. The interaction between BSA with Cu^{II}–SCNP1 or Cu^{II}–SCNP2 was measured by using STD spectroscopy,²⁴ which uses the nuclear Overhauser effect (NOE) to assess the nature of possible intermolecular interactions. The nanoparticles were mixed with BSA in 1:1 molar ratio in deuterated PBS buffer, and the STD

spectra were acquired by irradiating the mixture at 7.0 ppm, the protein aromatic region. The STD signals corresponding to the trimethyl ammonium on SCNP1, the PEG groups on SCNP2 and the hydrophobic alkyl chains for both SCNPs were measured and the % STD calculated. As shown in Fig. 2b, the PEG and hexamethylene groups on SCNP2 showed negligible and weaker STD signals, respectively with BSA. The magnitude of these differences is significant and consistent with weaker interactions.^{25,26}

To further examine the potential interaction with proteins, a fluorescence anisotropy experiment was performed using fluorescein labeled BSA. As seen in Fig. 2c, SCNP2 exhibited significantly lower polarization values than SCNP1. To assess the significance of this difference, the polarization of the SCNP1·BSA complex was reexamined with increasing sodium chloride concentration to lower the electrostatic binding (Figure S4). The reduced polarization is similar to that see in SCNP2 and supports the reduced adhesion afforded by the PEG shell.

Protein vs. small molecule CuAAC activity. To test whether the PEG shell in SCNP2 with its lower protein association translates into reduced uptake or attach mode catalysis, the rates of the CuAAC click reaction between Al1 and alkynylated BSA (BSA-Al) were measured. BSA-Al was prepared by reacting BSA with the NHS-ester of 4-pentynoic acid, the protein product containing on average 13 alkyne groups as indicated by MALDI-MS. To monitor the reactions at low concentration, a fluorogenic azido coumarin (Az1) was used as the azide substrate. Thus, Az1 exhibits a large increase in fluorescence after the click reaction. Fluorogenic reactions were performed in PBS buffer containing Az1 (20 μ M) with Al1 (40 μ M) or BSA-Al (2 μ M) by using either CuI-SCNP1 (2 μ M) or CuI-SCNP2 (2 μ M). For reference, one of the fastest known small molecule catalysts CuI-BTTAA (20 μ M) was used at the same copper concentration.

Cu^I-SCNP1 and Cu^I-SCNP2 both showed high efficiency in catalyzing the click reaction between the small molecules Az1 and

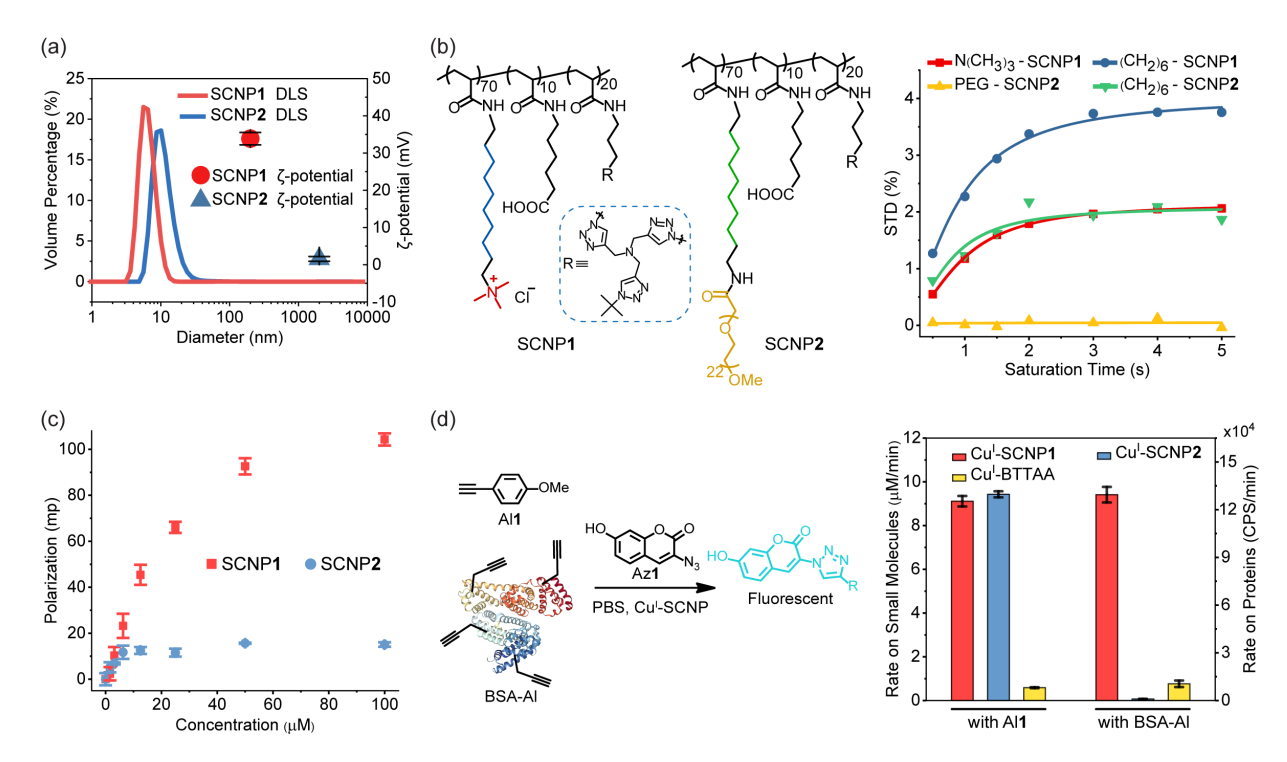


Figure 2. (a) DLS and ζ-potential data of SCNP1 and SCNP2. (b) STD signal intensities of the trimethyl ammonium groups and alkyl chains on 100 μ M Cu^{II}–SCNP1 or Cu^{II}–SCNP2 with 100 μ M BSA in deuterated PBS buffer (1x, pD = 7.4) irradiated at 7.0 ppm. Trimethyl ammonium group and hydrophobic chains labelled with colors used in STD plot. (c) Fluorescence polarization of fluorescein labelled BSA (2 μ M) with different concentration of Cu^{II}–SCNP1 or Cu^{II}–SCNP2 in PBS buffer (1x, pH = 7.4). (d) Initial reaction rates for small molecule and protein substrates with Cu^{II}–SCNP1 (2 μ M) or Cu^{II}–SCNP2 (2 μ M) in PBS buffer (1x, pH = 7.4) at room temperature. For small molecule substrate: Al1 (40 μ M) and Az1 (20 μ M). For protein substrate: BSA-Al (2 μ M) and Az1 (40 μ M). Error bars represent the standard deviation of three independent experiments. Data for SCNP1 and BTTAA from ref. 20.

Al1. Thus, both nanoparticles achieved >90% conversion within 5 min (Figure S2a), and their initial rates were around 15 times faster than that of Cu¹–BTTAA (Figure 2d).²³ As previously observed, Cu¹–SCNP1 exhibited a high rate of reaction in protein labeling, performing the click reaction between BSA-Al and Az1 12-fold faster than Cu¹–BTTAA. However, Cu¹–SCNP2 failed to catalyze the reactions on BSA-Al, exhibiting an 11 and 137-fold slower rate than that of Cu¹–BTTAA or Cu¹-SCNP1, respectively. The fluorogenic reactions were also performed on a mixture of Al1 and BSA-Al, and Cu¹–SCNP2 showed a 60-fold preference for the small molecule over the protein (Figure S2b). These results suggest that the PEG groups on the clickase block its active sites for protein substrates, while maintaining the capability to uptake and catalyze click reactions with small molecule substrates.

Protein-ligand binding study. Uptake mode catalysis by Cu^I–SCNP requires the nanoparticle to bind small molecules within their interior, the binding constants estimated to be in the micromolar range. ^{16,20} If a protein binds a small molecule azide or alkyne with a comparable or lower *K*_D, its uptake mode click reaction would be inhibited, but only if attach mode is not operative (Figure 3a). The demonstration that the PEG groups in Cu^I–SCNP1 prevent its interaction with proteins raises the interesting possibility that the nanoparticle might be used to screen for small molecules that are bound to proteins of interest. To test this hypothesis, fluorogenic reactions were performed between Az1 and seven alkyne substrates with or without adding carbonic anhydrase II.

Carbonic anhydrase II (CA) was chosen as an inexpensive, readily available, and prevalent enzyme. Its inhibitors were once commonly used therapeutic agents, but now are limited mostly to glaucoma treatment. The proof of principle screen for CA binders used a reactivity index to estimate the small molecule binding capability. The reactivity index is defined as the ratio of the initial

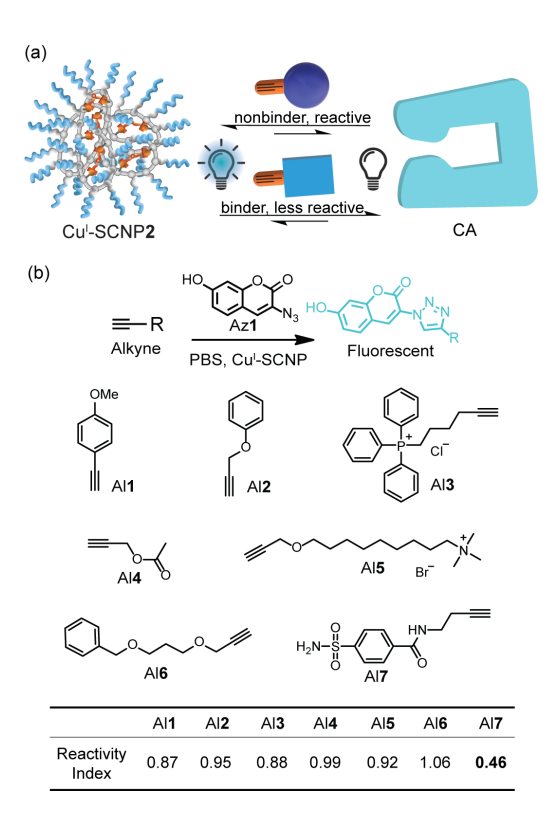


Figure 3. Protein-ligand binding study by using Cu^I-SCNP**2**. (a) Illustration of competitive binding with proteins making nanoparticle only active on free substrates. (b) Chemical structure of alkyne substrates and their reactivity index. Fluorogenic reactions in PBS buffer: [Cu^I-SCNP**2**] = $4 \mu M$, [Az**1**] = $2 \mu M$, [NaAsc] = $200 \mu M$ and [Al] = $1 \mu M$ with/without [CA] = $2 \mu M$.

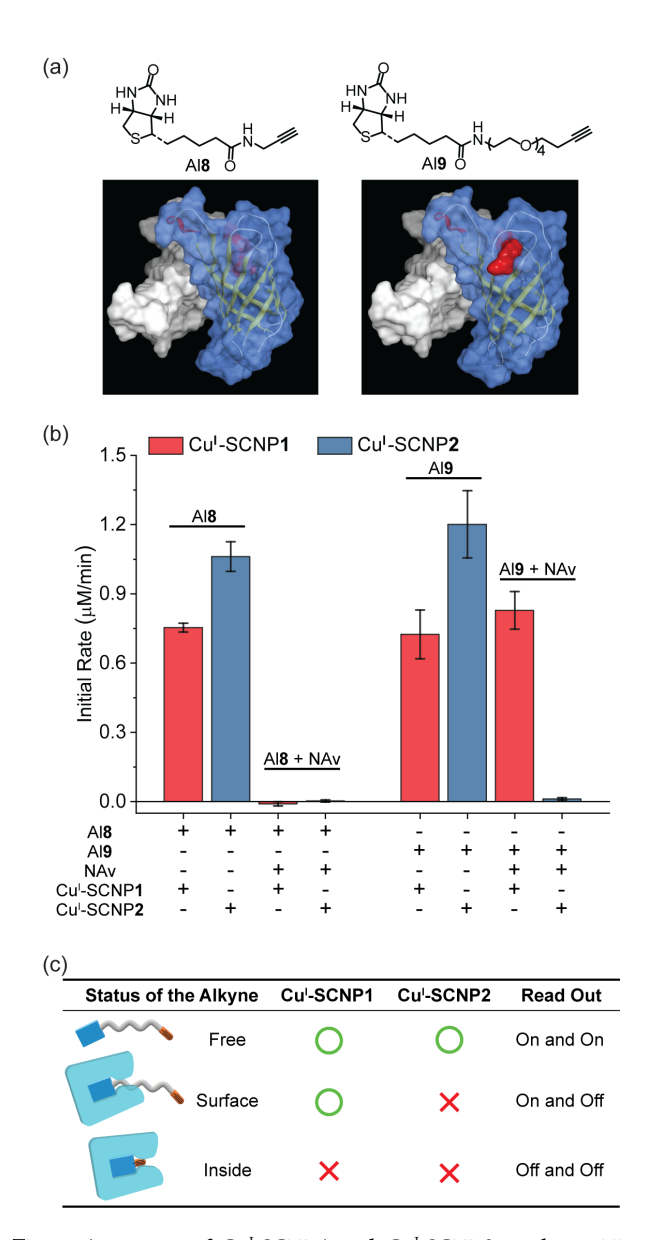


Figure 4. Activity of Cu^I-SCNP1 and Cu^I-SCNP2 on biotin-NAv complexes. (a) The chemical structures of two alkyne functionalized biotin compounds and the MOE simulation results of NAv-Al8 and NAv-Al9 complexes. (b) The initial reaction rates of fluorogenic reactions conducted in PBS buffer containing: [Cu^I-SCNP] = 4 μ M, [Az1] = 2 μ M, [NaAsc] = 200 μ M and [AI] = 1 μ M with/without [CA] = 2 μ M. The error bars represent the standard deviation of three independent experiments. (c) Schematic illustration of the SCNP mediated fluorogenic protein-ligand binding assay.

rate of the click reaction with CA to that without CA. If an alkyne substrate binds to CA, it would become less accessible to Cu¹-SCNP**2**, producing a reactivity index lower than 1. If there is no interaction between the substrate and protein, the index should remain around 1, because the small molecule is free in solution to be taken up into the nanoparticle interior for the click reaction. As shown in Figure 3b, Al**1-6** exhibited reactivity index closed to 1, indicating they were nonbinding or weakly bound to CA. Al**7** was used because sulfamoyl compounds are known CA inhibitors.²⁸ Indeed, its reactivity index was significantly lower.

The activity of Cu^I–SCNP1 and Cu^I–SCNP2 toward proteinligand complexes was studied in more detail. Thus, two biotinalkyne derivatives that bind to neutravidin (NAv) tightly were prepared with either a short (Al8) or a long linker (Al9) (Figure 4a). NAv is the deglycosylated form of avidin and exhibits a neutral surface charge. The crystal structure of the Nav-biotin complex was obtained from the protein data bank (PDB, ID: 2AVI) and imported into the molecular operating environment (MOE) software. The biotin structure in the protein was mutated into Al8 or Al9 using the build feature in MOE, and the structure underwent energy minimization. Shown in Figure 4a are two identical subunits of NAv, one colored blue and the ligands colored red. For the NAv-Al8 complex, the whole Al8 substrate was buried inside the protein, whereas in NAv-Al9, the linker chain reaches out to the protein surface allowing the alkyne group to be accessed.

The initial rates of the CuAAC click reaction between Az1 and either free ligands Al8 and Al9 or bound ligands NAv-Al8 or NAv-Al9 catalyzed by Cu^I-SCNP1 and Cu^I-SCNP2 were measured. As shown in Figure 4b, both nanoparticles behaved similarly with free and bound Al8. Thus, free ligand Al8 reacts in uptake mode, but the neutravidin-bound Al8 is inaccessible. Even with the longer linker group in NAv-Al9, Cu^I-SCNP2 showed almost no activity in the click reaction with Az1, consistent with the observation that only free small molecules are reactive toward the PEGylated nanoparticle. These results indicate that protein-ligand binding can be assessed by using the two nanoparticles as the dual logical gates. As shown in Figure 4c, the assay would be conducted by performing fluorogenic reactions with Cu^I-SCNP1 and Cu^I-SCNP2 separately. The protein ligand interactions can be assessed via the fluorescence readout with three possibilities: free (on and on), on the protein surface and accessible (on and off) or bound to the protein interior and inaccessible (off and off).

Recently, proteolysis targeting chimera (PROTAC) technology has received considerable attention because of its potential to degrade pathogenic proteins and particularly to treat diseases originating from "undruggable" proteins, those for which a traditional inhibitor strategy is not available.²⁹ PROTAC ligands typically contain two different protein binding groups on each end of a linker, and thus are able to bring together the target protein and the protein degradation machinery. However, PROTAC binding is highly dependent on the environment and concentrations, and some suffer from the "hook effect," resulting in poor conjugation of the two proteins.³⁰ Thus, evaluating the binding status of both endgroup ligands is essential in developing PROTAC ligands.

A PROTAC-inspired model compound, Al10, was synthesized with a biotin ligand and a sulfamoyl group for targeting for NAv and CA, respectively as well as an alkyne group adjacent to each binding moiety. In the absence of proteins, both Cu^I-SCNP1 and Cu^I-SCNP2 catalyzed the click reaction between Al10 and Az1 as was observed by a fluorescence increase (on and on). Upon adding NAv, Cu^I-SCNP1 remained active exhibiting a reactivity index of ca. 1.2, whereas Cu^I-SCNP2 showed almost no activity (Figure 5). This on and off fluorescence readout suggests that Al10 was bound to NAv, most likely with the alkyne group next to the biotin group buried inside the protein scaffold and the other alkyne group exposed on the surface. When both NAv and CA were added to Al10, Cu^I-SCNP2 remained inactive, whereas the initial rate of Cu^I-SCNP1 decreased only ca. 20% (off and mostly on), indicating that the alkyne group on the sulfamoyl side remained partly available to Cu^I-SCNP1. This observation suggests that in the presence of both proteins there is an equilibrium mixture of CA-Al10-NAv and Al10-NAv. Overall, this model experiment demonstrates the potential use of Cu^I-SCNP1 and Cu^I-SCNP2 in a combination fluorogenic assay to test potential PROTAC ligands.

Cu^I-SCNP2 mediated extracellular synthesis and drug screening. Given the weak protein absorption, we wondered whether SCNP2,

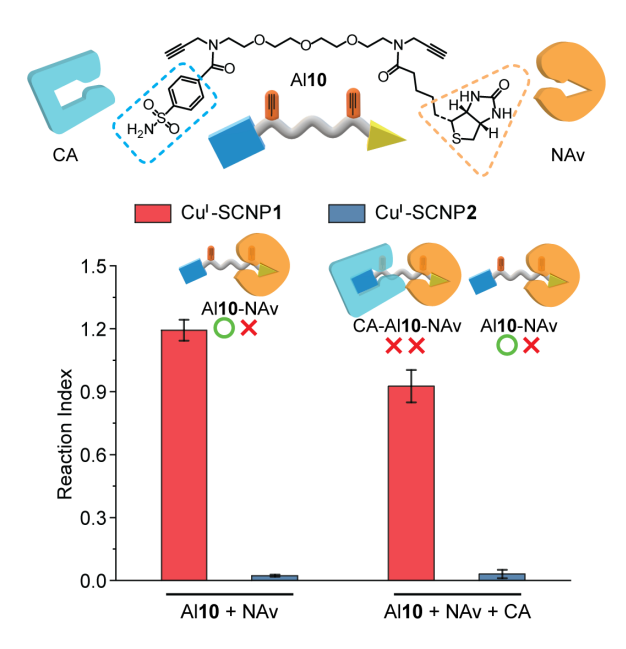


Figure 5. The chemical structure of Al**10** and the illustration of its binding towards CA and NAv. The initial reaction rates of fluorogenic reactions conducted in PBS buffer containing: [Cu¹-SCNP**2**] or [Cu¹-SCNP**2**] = 4 μ M, [Az**1**] = 2 μ M, [NaAsc] = 200 μ M and [Al] = 1 μ M with/without [NAv] = 0.4 μ M or [CA] = 2 μ M. The error bars represent the standard deviation of six independent experiments.

unlike SCNP1 might reside extracellularly thereby allowing drug synthesis and screening without the nanoparticle potentially affecting the intracellular environment. Albertazzi and Palmans reported that catalytic Jeffamine-based SCNP could be kept largely in the extracellular space under certain conditions. 19 Therefore, the cytotoxicity and cell permeability of the SCNP were investigated. Using HeLa cells, SCNP2 was found to exhibit significant cytotoxicity at concentrations $\geq 8 \mu M$ (Fig. S3). The uptake was assessed by labelling both SCNP1 and SCNP2 with Cy5 (see Supporting Information for details). HeLa cells were incubated in the DMEM media (10% FBS added) containing 2 µM of Cu^{II}-SCNP1-Cy5 or Cu^{II}-SCNP2-Cy5 for 24 h. As shown in Figure 6a, the red fluorescence within the cells indicated Cu^{II}-SCNP1-Cy5 was taken up, whereas almost no fluorescence was found intracellularly when the HeLa cells were treated with Cu^{II}-SCNP2-Cy5. This observation confirms that under these conditions SCNP2 is "nonsticky" and exhibits poor cell penetration.

To test whether the extracellular catalyst is active and can produce small molecule products that can subsequently enter the cell through passive diffusion (Figure 6b),³¹ the fluorogenic click reaction between Az1 and Al1 was performed with HeLa cells and Cu¹-SCNP2 in PBS buffer. A concentration of 500 nM was used that is below the concentration where a similar Jeffamine-based SCNP remained in the extracellular space for several hours.¹⁹ As shown in Figure 6c, after the reaction initiation by adding NaAsc, the fluorescence intensity of the HeLa cells gradually increased and reached the maximum in about 10 min. This result suggests that although the nanoparticle cannot penetrate the cell membrane, its reaction products readily diffuse inside the cells.

Click chemistry has been successfully applied to drug screening because it can generate a large number of compounds in high yields. ^{32,33} Recently, by using "SuFEx" click chemistry, ³⁴ Dong and Sharpless reported a method to convert primary amines into azido

groups which could subsequently react with alkynes to generate a large library.³⁵ The relatively low activity of traditional copper catalysts means that the CuAAC reactions are typically performed at millimolar concentration of substrates and catalysts, thereby requiring an organic solvent to solubilize the reagents. Thus, the products are purified and subsequently transferred to cells to test their bioactivity. The bioorthogonality and high activity of the Cu¹-SCNP2 clickase provides an opportunity for in situ drug synthesis, streamlining the screening. In particular, the ability to obtain near quantitative yields of click products at micromolar concentrations²⁰ is important because this is the effective concentration range of many anticancer agents.

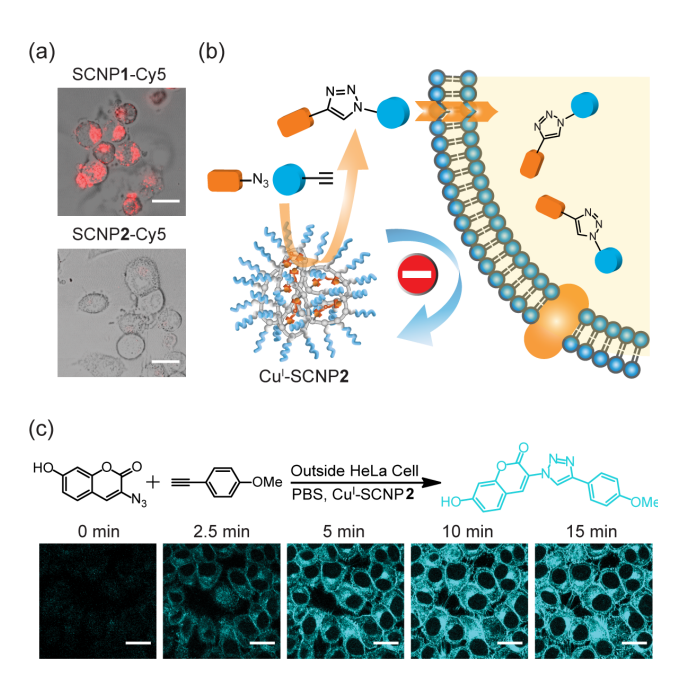


Figure 6. Cell uptake ability of SCNPs and extracellular synthesis. (a) The confocal images of HeLa cells incubated with 2 μM of Cu^{II}-SCNP1-Cy5 or Cu^{II}-SCNP2-Cy5 for 24 h in DMEM media (10% FBS added). (b) Schematic illustration of extracellular CuAAC synthesis where the nanoparticle stayed outside the cells and the reaction products defused in. (c) The confocal images over time of fluorogenic reaction outside HeLa cells performed in PBS buffer containing: [Cu^I-SCNP2] = 1 μM, [Az1] = 20 μM, [Al1] = 20 μM and [NaAsc] = 200 μM.

The proof of concept, anticancer agent screening method developed is based on the in situ, extracellular click reaction between 10 azido substrates (Az2-11) and 6 alkyne substrates (Al1-6). Screening of the 60 possible triazole products was performed by using a 96 wells plate with HeLa cells in a fast and high-throughput manner. To each well was added 50 μL of PBS buffer containing [Cu^I-SCNP2] = 1 μM , [Az] = 40 μM , [Al] = 40 μM and [NaAsc] = 100 μM , and the reaction was allowed to proceed outside the cell for 30 min, long enough for full conversion (Figure S8). To each well was added 50 µL of DMEM media (10% FBS), and the cells were incubated for 24 h. The cell viability was measured by using the MTT assay, the results presented in Figure 7. Different levels of cytotoxicity were observed for the screened compounds, the most of toxic compounds were the derivatives of triphenyl phosphonium, phenyl methoxy compound and colchicine. We chemically synthesized and purified click product Al3-Az3, and its cytotoxicity towards HeLa cells was studied more carefully. Thus, a dose-dependent cytotoxicity was observed with an IC₅₀ = $24 \mu M$, consistent with the screening result (Figure S10). The toxicity of this compound likely arises because the triphenyl phosphonium group (Al3)

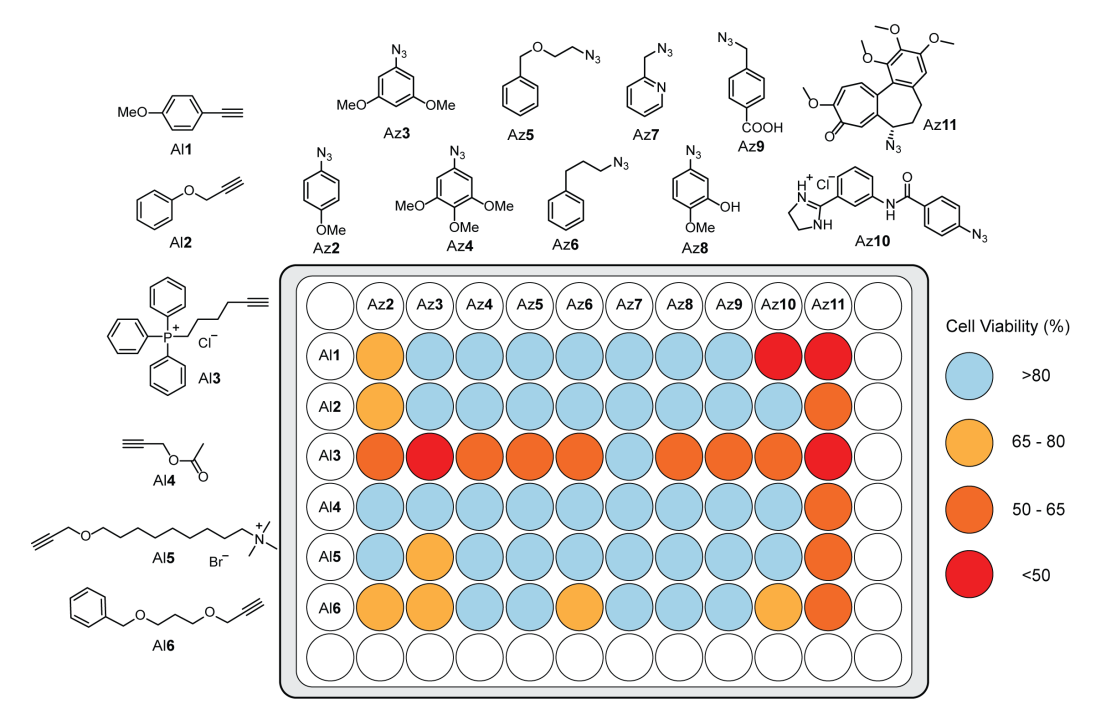


Figure 7. Cu^I-SCNP**2** mediated CuAAC synthesis and drug screening extracellularly. The chemical structures of the substrates and their numbering are presented. Reactions were performed outside HeLa cells in a 96 wells plate, where the PBS buffer contained: [Cu^I-SCNP**2**] = 1 μ M, [Az] = 40 μ M, [Al] = 40 μ M and [NaAsc] = 100 μ M. The data was presented as duplicated experiments.

brings the phenyl methoxy unit (Az $\bf 3$) into cell mitochondria and disrupts its function. $^{36\cdot38}$

■ CONCLUSION

We previously demonstrated the high CuAAC activity of CuI-SCNP1 in performing the click reaction between small molecules (uptake mode). Surprisingly the utility of this catalyst extended to protein surface reactions because of the unexpected discovery of an "attach mode" wherein the SCNP binds protein surfaces using both electrostatic and hydrophobic interactions. Although this added functionality can be useful, it limits some potential applications. The Cu^I-SCNP2 clickase developed here, retains the high reactivity and selectivity in performing the CuAAC (click) reaction on small molecules, but its PEGylated shell serves as a protein and cell membrane gate. Thus, the bioorthogonal click reaction is performed by a polymeric catalyst that is itself bioorthogonal. This new selectivity enables a fluorescent assay for studying protein-ligand binding, with Cu^I-SCNP1 and Cu^I-SCNP2 acting in combination as a dual logical gate. The PEG groups also prevent the cell uptake of the nanoparticle. As a result, Cu^I-SCNP2 resides extracellularly and serves as a nanoscale factory to produce bioactive compounds in situ at the low concentrations often used in bioassays. The application to a potential anticancer agent screening method was demonstrated. More broadly, this work points to the utility of synthetic polymers as artificial enzymes with versatile, non-natural functions for bioapplications.

ASSOCIATED CONTENT

Supporting Information.

The Supporting Information is available free of charge at:

General experimental procedures and detailed synthetic procedures and characterization data for small molecules and polymers, and additional kinetic data along with details of the computational methods (PDF)

AUTHOR INFORMATION

Corresponding Author

Steven C. Zimmerman - Department of Chemistry, Center for Biophysics and Quantitative Biology, University of Illinois, Urbana, Illinois 61801, United States; orcid.org/0000-0002-5333-3437; Email: sczimmer@illinois.edu.

Authors

Junfeng Chen - Department of Chemistry, University of Illinois, Urbana, Illinois 61801, United States; orcid.org/0000-0002-7100-0839

Ke Li - Department of Chemistry, University of Illinois, Urbana, Illinois 61801, United States, orcid.org/0000-0003-3851-7710 Sarah E. Bonson - Department of Chemistry, University of Illinois

Sarah E. Bonson - Department of Chemistry, University of Illinois, Urbana, Illinois 61801, United States; orcid.org/0000-0003-4167-3730

Complete contact information is available at: https://

Notes

The authors declare no competing financial interest.

ACKNOWLEDGMENT

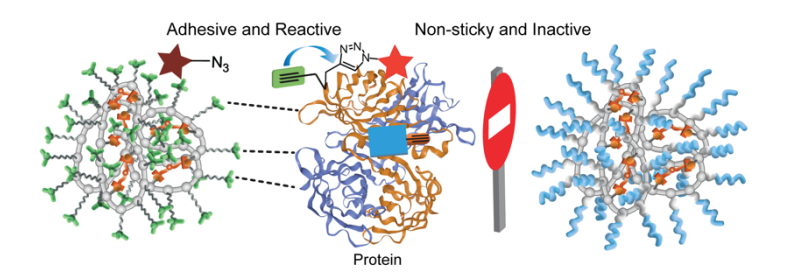
This work was supported by the National Science Foundation (NSF CHE-1709718, NSF GRFP DGE-1746047) and the National Institutes of Health (R01 AR069645).

REFERENCES

(1) Tonga, G. Y.; Jeong, Y.; Duncan, B.; Mizuhara, T.; Mout, R.; Das, R.; Kim, S. T.; Yeh, Y.-C.; Yan, B.; Hou, S.; Rotello, V. M., Supramolecular regulation of bioorthogonal catalysis in cells using nanoparticle-embedded transition metal catalysts. *Nat. Chem.* **2015**, *7*, 597-603.

- (2) Brevé, T. G.; Filius, M.; Araman, C.; van der Helm, M. P.; Hagedoorn, P.-L.; Joo, C.; van Kasteren, S. I.; Eelkema, R., Conditional Copper-Catalyzed Azide–Alkyne Cycloaddition by Catalyst Encapsulation. *Angew. Chem. Int. Ed.* **2020**, *59*, 9340-9344.
- (3) Kaphan, D. M.; Levin, M. D.; Bergman, R. G.; Raymond, K. N.; Toste, F. D., A supramolecular microenvironment strategy for transition metal catalysis. *Science* **2015**, *350*, 1235-1238.
- (4) Yang, Q.; Xu, Q.; Jiang, H.-L., Metal–organic frameworks meet metal nanoparticles: synergistic effect for enhanced catalysis. *Chem. Soc. Rev.* **2017**, *46*, 4774-4808.
- (5) Blackman, L. D.; Varlas, S.; Arno, M. C.; Houston, Z. H.; Fletcher, N. L.; Thurecht, K. J.; Hasan, M.; Gibson, M. I.; O'Reilly, R. K., Confinement of Therapeutic Enzymes in Selectively Permeable Polymer Vesicles by Polymerization-Induced Self-Assembly (PISA) Reduces Antibody Binding and Proteolytic Susceptibility. *ACS Cent. Sci.* 2018, 4, 718-723.
- (6) Rubio-Cervilla, J.; González, E.; Pomposo, J., Advances in Single-Chain Nanoparticles for Catalysis Applications. *Nanomaterials* **2017**, *7*, 341-360.
- (7) Mavila, S.; Eivgi, O.; Berkovich, I.; Lemcoff, N. G., Intramolecular Cross-Linking Methodologies for the Synthesis of Polymer Nanoparticles. *Chem. Rev.* **2016**, *116*, 878-961.
- (8) Ouchi, M.; Badi, N.; Lutz, J.-F.; Sawamoto, M., Single-chain technology using discrete synthetic macromolecules. *Nat. Chem.* **2011**, *3*, 917-924.
- (9) Huurne, G. M. t.; Palmans, A. R. A.; Meijer, E. W., Supramolecular Single-Chain Polymeric Nanoparticles. CCS Chemistry 2019, 1, 64-82.
- (10) Chen, J.; Garcia, E. S.; Zimmerman, S. C., Intramolecularly Cross-Linked Polymers: From Structure to Function with Applications as Artificial Antibodies and Artificial Enzymes. *Acc. Chem. Res.* **2020**.
- (11) Cole, J. P.; Hanlon, A. M.; Rodriguez, K. J.; Berda, E. B., Proteinlike structure and activity in synthetic polymers. *J. Polym. Sci., Part A: Polym. Chem.* **2017**, *55*, 191-206.
- (12) Pomposo, J. A., Ed. Single-Chain Polymer Nanoparticles: Synthesis, Characterization, Simulations, and Applications; John Wiley & Sons, 2017.
- (13) Terashima, T.; Mes, T.; De Greef, T. F. A.; Gillissen, M. A. J.; Besenius, P.; Palmans, A. R. A.; Meijer, E. W., Single-Chain Folding of Polymers for Catalytic Systems in Water. *J. Am. Chem. Soc.* **2011**, *133*, 4742-4745.
- (14) Liu, Y.; Pauloehrl, T.; Presolski, S. I.; Albertazzi, L.; Palmans, A. R. A.; Meijer, E. W., Modular Synthetic Platform for the Construction of Functional Single-Chain Polymeric Nanoparticles: From Aqueous Catalysis to Photosensitization. *J. Am. Chem. Soc.* **2015**, *137*, 13096-13105.
- (15) Huerta, E.; Stals, P. J. M.; Meijer, E. W.; Palmans, A. R. A., Consequences of Folding a Water-Soluble Polymer Around an Organocatalyst. *Angew. Chem.* **2013**, *125*, 2978-2982.
- (16) Chen, J.; Wang, J.; Bai, Y.; Li, K.; Garcia, E. S.; Ferguson, A. L.; Zimmerman, S. C., Enzyme-like Click Catalysis by a Copper-Containing Single-Chain Nanoparticle. *J. Am. Chem. Soc.* **2018**, *140*, 13695-13702.
- (17) Bai, Y.; Feng, X.; Xing, H.; Xu, Y.; Kim, B. K.; Baig, N.; Zhou, T.; Gewirth, A. A.; Lu, Y.; Oldfield, E.; Zimmerman, S. C., A Highly Efficient Single-Chain Metal–Organic Nanoparticle Catalyst for Alkyne–Azide "Click" Reactions in Water and in Cells. *J. Am. Chem. Soc.* **2016**, *138*, 11077-11080.
- (18) Chen, J.; Li, K.; Shon, J. S. L.; Zimmerman, S. C., Single-Chain Nanoparticle Delivers a Partner Enzyme for Concurrent and Tandem Catalysis in Cells. *J. Am. Chem. Soc.* **2020**, 142, 4565-4569.
- (19) Liu, Y.; Pujals, S.; Stals, P. J. M.; Paulöhrl, T.; Presolski, S. I.; Meijer, E. W.; Albertazzi, L.; Palmans, A. R. A., Catalytically Active Single-Chain Polymeric Nanoparticles: Exploring Their Functions in Complex Biological Media. *J. Am. Chem. Soc.* **2018**, *140*, 3423-3433.
- (20) Chen, J.; Wang, J.; Li, K.; Wang, Y.; Gruebele, M.; Ferguson, A. L.; Zimmerman, S. C., Polymeric "Clickase" Accelerates the Copper

- Click Reaction of Small Molecules, Proteins, and Cells. J. Am. Chem. Soc. 2019, 141, 9693-9700.
- (21) Kolb, H. C.; Finn, M. G.; Sharpless, K. B., Click Chemistry: Diverse Chemical Function from a Few Good Reactions. *Angew. Chem. Int. Ed.* **2001**, *40*, 2004-2021.
- (22) Blümmel, J.; Perschmann, N.; Aydin, D.; Drinjakovic, J.; Surrey, T.; Lopez-Garcia, M.; Kessler, H.; Spatz, J. P., Protein repellent properties of covalently attached PEG coatings on nanostructured SiO2-based interfaces. *Biomaterials* **2007**, *28*, 4739-4747.
- (23) Besanceney-Webler, C.; Jiang, H.; Zheng, T.; Feng, L.; Soriano del Amo, D.; Wang, W.; Klivansky, L. M.; Marlow, F. L.; Liu, Y.; Wu, P., Increasing the Efficacy of Bioorthogonal Click Reactions for Bioconjugation: A Comparative Study. *Angew. Chem. Int. Ed.* **2011**, *50*, 8051-8056.
- (24) Mayer, M.; Meyer, B., Characterization of Ligand Binding by Saturation Transfer Difference NMR Spectroscopy. *Angew. Chem. Int. Ed.* **1999**, *38*, 1784-1788.
- (25) Vasile, F.; Menchi, G.; Lenci, E.; Guarna, A.; Potenza, D.; Trabocchi, A., Insight to the binding mode of triazole RGD-peptidomimetics to integrin-rich cancer cells by NMR and molecular modeling. *Biorg. Med. Chem.* **2016**, *24*, 989-994.
- (26) Neffe, A. T.; Bilang, M.; Meyer, B., Synthesis and optimization of peptidomimetics as HIV entry inhibitors against the receptor protein CD4 using STD NMR and ligand docking. *Org. Biomol. Chem.* **2006**, *4*, 3259-3267.
- (27) Sivakumar, K.; Xie, F.; Cash, B. M.; Long, S.; Barnhill, H. N.; Wang, Q., A Fluorogenic 1,3-Dipolar Cycloaddition Reaction of 3-Azidocoumarins and Acetylenes. *Org. Lett.* **2004**, *6*, 4603-4606.
- (28) Supuran, C. T., Carbonic anhydrases: novel therapeutic applications for inhibitors and activators. *Nat. Rev. Drug Discov.* **2008**, *7*, 168-181.
- (29) Sakamoto, K. M.; Kim, K. B.; Kumagai, A.; Mercurio, F.; Crews, C. M.; Deshaies, R. J., Protacs: Chimeric molecules that target proteins to the Skp1–Cullin–F box complex for ubiquitination and degradation. *Proc. Natl. Acad. Sci.* **2001**, *98*, 8554-8559.
- (30) An, S.; Fu, L., Small-molecule PROTACs: An emerging and promising approach for the development of targeted therapy drugs. *EBioMedicine* **2018**, *36*, 553-562.
- (31) Clavadetscher, J.; Hoffmann, S.; Lilienkampf, A.; Mackay, L.; Yusop, R. M.; Rider, S. A.; Mullins, J. J.; Bradley, M., Copper Catalysis in Living Systems and In Situ Drug Synthesis. *Angew. Chem. Int. Ed.* **2016**, *55*, 15662-15666.
- (32) Kolb, H. C.; Sharpless, K. B., The growing impact of click chemistry on drug discovery. *Drug Discov. Today* **2003**, *8*, 1128-1137.
- (33) Thirumurugan, P.; Matosiuk, D.; Jozwiak, K., Click Chemistry for Drug Development and Diverse Chemical–Biology Applications. *Chem. Rev.* **2013**, *113*, 4905-4979.
- (34) Dong, J.; Krasnova, L.; Finn, M. G.; Sharpless, K. B., Sulfur(VI) Fluoride Exchange (SuFEx): Another Good Reaction for Click Chemistry. *Angew. Chem. Int. Ed.* **2014**, *53*, 9430-9448.
- (35) Meng, G.; Guo, T.; Ma, T.; Zhang, J.; Shen, Y.; Sharpless, K. B.; Dong, J., Modular click chemistry libraries for functional screens using a diazotizing reagent. *Nature* **2019**, *574*, 86-89.
- (36) Sabharwal, S. S.; Schumacker, P. T., Mitochondrial ROS in cancer: initiators, amplifiers or an Achilles' heel? *Nat. Rev. Cancer* **2014**, *14*, 709-721.
- (37) Pagliai, F.; Pirali, T.; Del Grosso, E.; Di Brisco, R.; Tron, G. C.; Sorba, G.; Genazzani, A. A., Rapid Synthesis of Triazole-Modified Resveratrol Analogues via Click Chemistry. *J. Med. Chem.* **2006**, *49*, 467-470.
- (38) Wang, F.; Zhang, Y.; Liu, Z.; Du, Z.; Zhang, L.; Ren, J.; Qu, X., A Biocompatible Heterogeneous MOF–Cu Catalyst for In Vivo Drug Synthesis in Targeted Subcellular Organelles. *Angew. Chem. Int. Ed.* **2019**, *58*, 6987-6992.



A Bioorthogonal Small Molecule Selective Polymeric "Clickase"

Junfeng Chen,[†] Ke Li,[†] Sarah E. Bonson,[†] and Steven C. Zimmerman*,^{†,‡}

Contents

Materials and Instruments	S2
Synthetic Procedures ·····	S3
Methods ···· S	S 11
Cell Study ····· S	315
References ····· S	S18

[†]Department of Chemistry, University of Illinois, Urbana, Illinois 61801, United States.

[‡]Center for Biophysics and Quantitative Biology, University of Illinois, Urbana, Illinois 61801, United States.

Materials and Instruments:

All reagents were purchased from Acros Organics, Fisher Scientific, Cambridge Chemical Technologies, Chem-Impex International, AK Scientific, TCI America, ProteinMods, AA block, or Sigma-Aldrich, and used without further purification unless otherwise noted. For the synthetic procedures, DCM, THF, acetonitrile, DMSO and DMF were stored over activated 4 Å molecular sieves. NMR spectra were recorded using Varian U500, Bruker CB500 or VNS750NB spectrometers in the NMR Laboratory, School of Chemical Science, University of Illinois. Spectra were processed by using MestReNova (v8.1). The chemical shift (δ) is listed in ppm and the coupling constants (*J*) are in Hz. Mass spectral analyses were provided by the Mass Spectrometry Laboratory, School of Chemical Science, University of Illinois, using ESI on a Waters Micromass Q-Tof spectrometer, FD on a Waters 70-VSE spectrometer. Transmission electron microscopy (TEM) was performed on a JEOL 2100 Cryo TEM, Materials Research Laboratory, University of Illinois at Urbana-Champaign. Fluorescence experiments were performed on a Horiba Fluoromax-4 fluorometer with FluorEssence (v3.5) software. Fluorescence polarization experiments were performed on an Analyst HT plate reader. Confocal microscopy studies were performed on a Leica SP8 UV/Visible Laser Confocal Microscope. The RAW data files were processed using OriginPro2019 and imported into Adobe Illustrator CC for coloring and annotation.

Synthetic Procedures

Synthesis of Di-Alkyne-PEG(3)

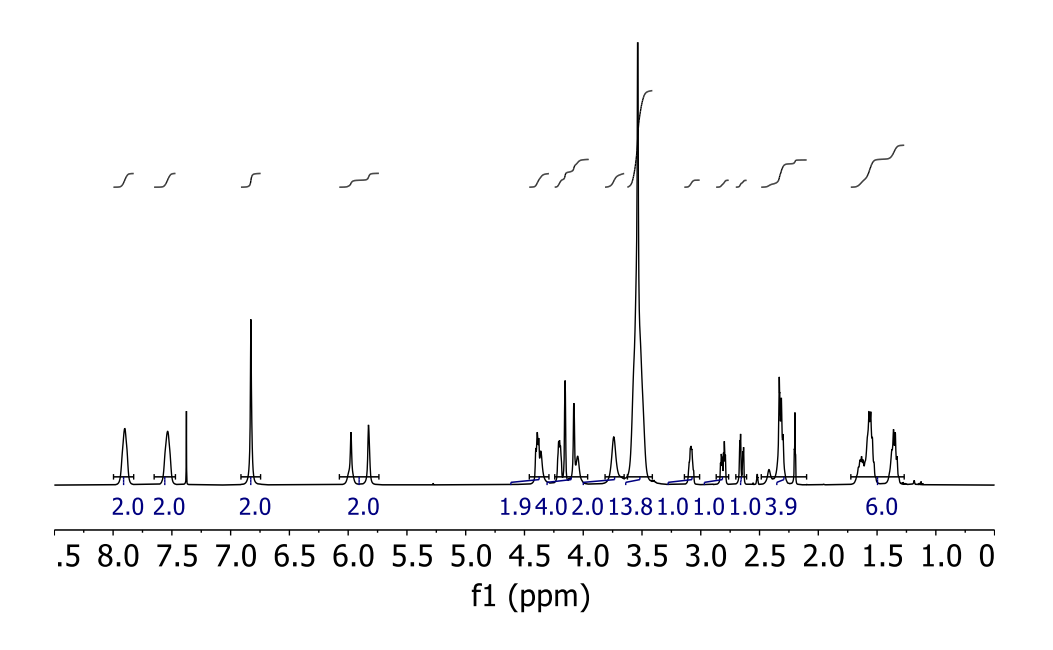
In a 20 mL glass vial, 500 mg (2.6 mmol) of **1** was suspended in 5 mL of SPS dried THF, and 1.36 g (6.2mmol) of (Boc)₂O was added with stirring. The mixture was stirred at room temperature for 12 h. To the mixture was added 1 mL of water, and the mixture was stirred for another 12 h. Volatiles were removed by using a rotary evaporator, and the crude product was dried under high vacuum. The crude **2** was used in the next step without further purification.

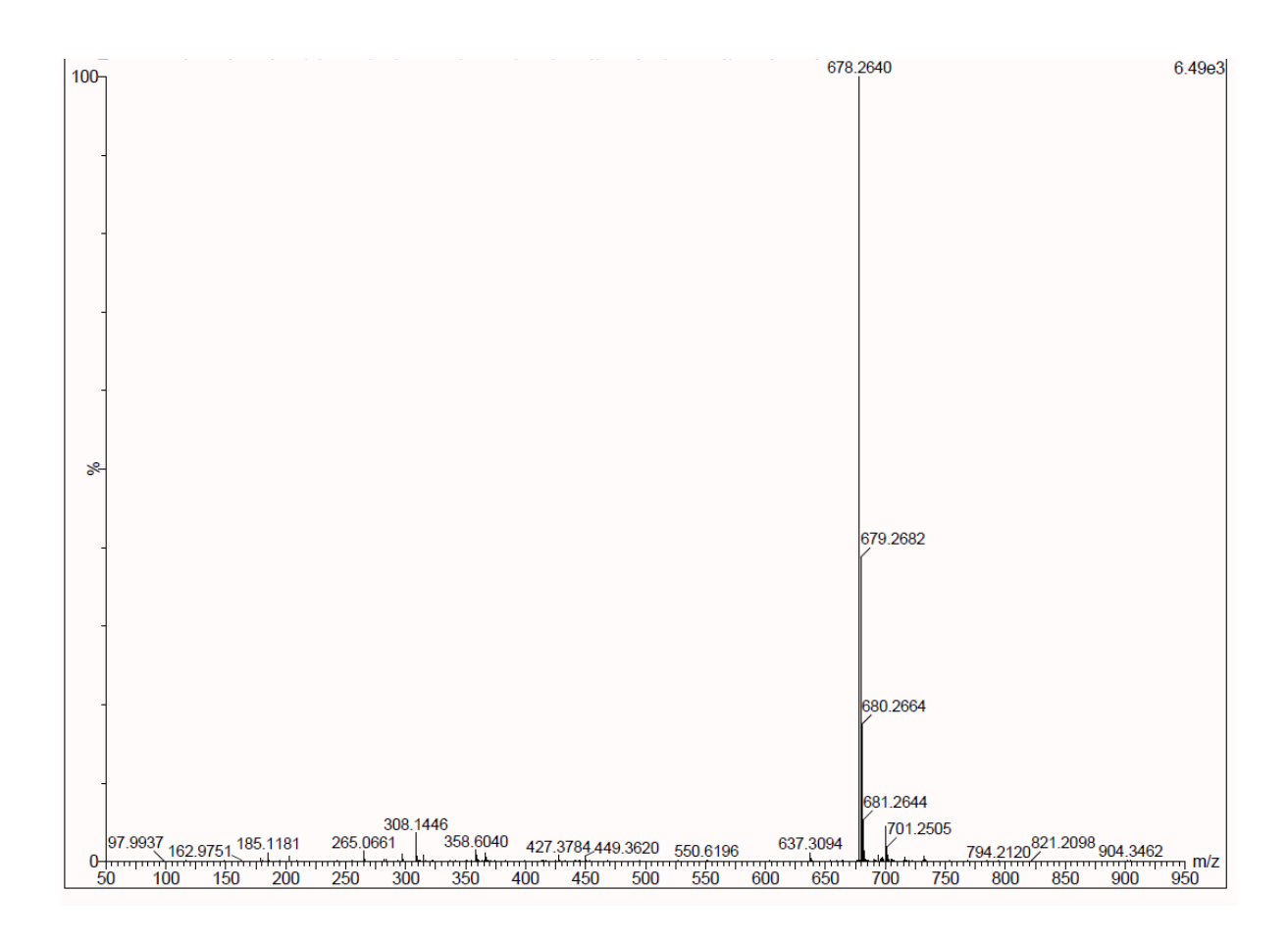
In a 300 mL round bottom flask, 2 from the last step was dissolved in 30 mL of SPS dried DMF and cooled in an ice bath. To the mixture was added 0.42 g (10.4 mmol) of NaH with fast stirring, and 1.55 g (10.4 mmol) of propargyl bromide (80 wt% in toluene) was added dropwise under N₂. The mixture was allowed to warm up to room temperature over roughly 30 min and stirred for 12 h. Volatiles were removed by using a rotary evaporator, and the mixture was suspended in 100 mL of saturated NH₄Cl(aq). The mixture was extracted twice with 50 mL of ethyl acetate, and the combined organic layer was washed with 100 mL of water and 50 mL of brine. The organic layer was dried over Na₂SO₄, filtered and concentrated by using a rotary evaporator. The crude product was purified by using silica column chromatography with a gradient from DCM to 30% (v/v) ethyl acetate in DCM to afford a brown gel-like solid. The resulting solid was redissolved in 3 mL of DCM and cooled in an ice bath. To the mixture was added 3 mL of TFA with stirring, and the mixture was allowed to warm up to room temperature over roughly 30 min and stirred for 6 h. Volatiles were removed by using a rotary evaporator, and 50 ml of toluene was added to the mixture and removed by using a rotary evaporator again. This process was repeated twice to afford 0.65 g (54%) of the title compound as a brown gel-like solid. ¹H NMR (500 MHz, CDCl₃): δ 9.22 (s, 4H), 3.87 (d, J = 2.8, 4H), 3.75 (t, J = 4.7, 4H), 3.58 (m, 8H), 3.30 (t, J = 5.4, 4H), 2.51 (t, J = 2.8, 4H). ¹³C NMR: (125 MHz, CDCl₃): δ 77.9, 72.7, 70.3, 70.1, 65.5, 46.0, 36.7. High resolution ESI-MS: m/z calculated for $C_{14}H_{25}N_2O_3$ ([M+H]⁺): 269.1865; found 269.1868.

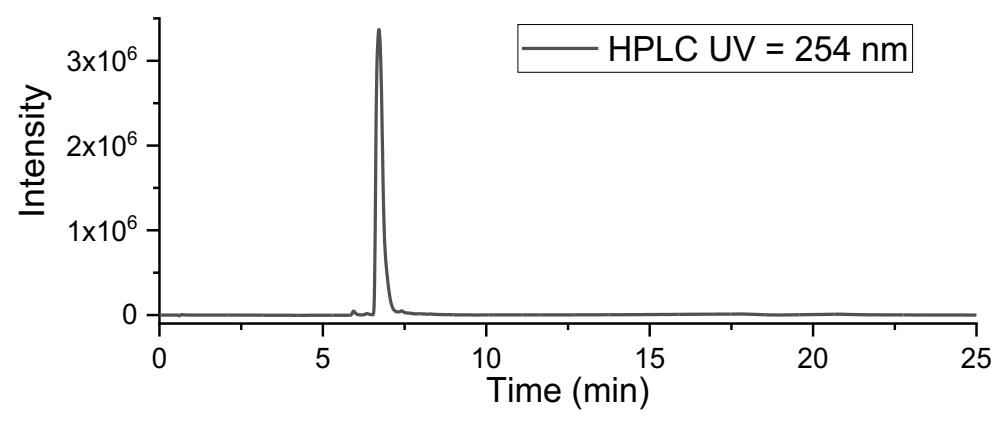
Synthesis of Dual-Protein-Binder (Al10)

In a 20 ml glass vial, 496 mg (1.0 mmol) of **3** and 258 mg (2.0 mmol) of DIPEA were dissolved in 1 mL of SPS dried DMF. In a separated vial, 417 mg (1.1 mmol) of HBTU, 149 mg (1.1 mmol) of HOBT, and 201 mg (1.0 mmol) of 4-sulfamolbenzoic acid were dissolved in 2 mL of SPS dried DMF, and the mixture was added to the **3** solution dropwise over 2 h at room temperature. The mixture was stirred at room temperature for additional 24 h. Volatiles were removed by using a rotary evaporator, and most of the impurities were removed by using reverse phase C18 column chromatography with a gradient from 100% water to 100% MeCN containing 10 mM HCl. The impure product **4** was used in the next step without further purification.

In a 20 mL glass vial, 230 mg (0.4 mmol) of crude **4** from the last step and 63 mg (490 mmol) of DIPEA were dissolved in a mixture of 1 mL of molecular sieve dried MeCN and 0.5 mL of SPS dried DMF. To the mixture was added biotin-NHS, and the mixture was stirred at 80 °C for 3 h. Volatiles were removed by using a rotary evaporator, and the mixture was purified by using a prep-HPLC with a gradient from 2% (v/v) MeCN in water to 100% MeCN containing 0.1% (v/v) TFA to afford 152 mg (22%) of the title compound as a white solid. High resolution ESI-MS: m/z calculated for $C_{31}H_{44}N_5O_8S_2$ ([M+H]⁺): 678.2631; found 678.2640. The results from ¹H NMR, HPLC and ESI-MS are shown below.







Synthesis of Al7

$$\begin{array}{c} \text{NH}_2 \\ \text{O=S=O} \\ \\ \text{O} \\$$

In a 200 mL round bottom flask, 1.0 g (5.0 mmol) of 4-sulfamolbenzoic acid, 1.4 g (7.5 mmol) of EDC-HCl and 0.96 g (7.5 mmol) of DIPEA were suspended in 50 mL of MeCN and the mixture was stirred at room temperature for 24 h. Volatiles were removed by using a rotary evaporator, and the crude product was purified by using silica column chromatography with a gradient from DCM to 5% v/v MeOH in DCM to afford 1.02 g (81%) of the title compound as a white solid. ¹H NMR (500 MHz, DMSO-d6): δ 8.83 (s, 1H), 7.99 (d, J = 8.5, 2H), 7.90 (d, J = 8.5, 2H), 7.48 (s, 2H), 3.41 (q, J = 5.6, 2H), 2.86 (t, J = 3.0, 1H), 2.46 (m, 2H). ¹³C NMR: (125 MHz, CDCl₃): δ 164.9, 146.8, 138.2, 128.3, 125.7, 83.4, 72.7, 38.9, 20.9. High resolution ESI-MS: m/z calculated for C₁₁H₁₃N₂O₃S ([M+H]⁺): 253.0647; found 253.0657.

Compound Al3 was prepared using the reported procedure.¹

Compound Al5 was prepared using the reported procedure.²

Compound Al6 was prepared using the reported procedure.³

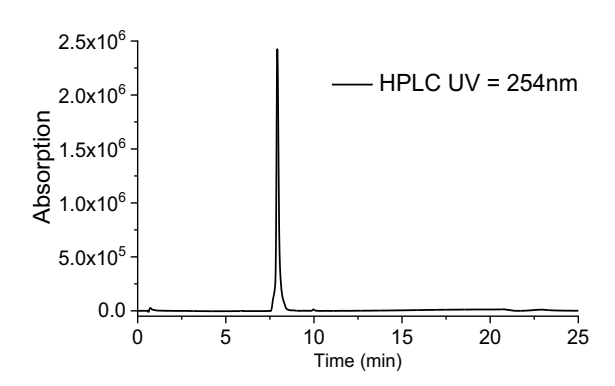
$$MeO$$
 OMe
 OMe
 OMe
 $Az3$
 $Az4$

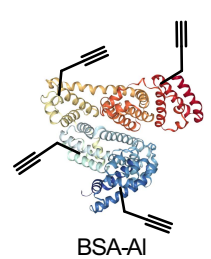
Compound Az3 and Az4 was prepared using the reported procedures.⁴

Compound Az8 was prepared using the reported procedure.⁵

Compound Az10 was prepared using the reported procedure.⁶

Compound Az11 was prepared as a 10 mM solution in DMSO using the reported procedure.⁷ The result from HPLC is shown below.





BSA-Al was prepared using the reported procedure.³

Synthesis of Anticancer Compound Al3-Az3

In a 20 mL glass vial, 102 mg (0.27 mmol) of Al**3** and 72 mg (0.40 mmol) of Az**3** were suspended in 2 ml of water containing [Cu^I-SCNP**1**] = 100 μ M and [NaAsc] = 20 mM. The mixture was stirred at 40 °C for 2 h. To the mixture was added 3 mL of DCM, and the organic layer was separated and purified by using silica column chromatography with a gradient from DCM to 10% MeOH in DCM to afford 133 mg (89%) of the title compound as a white solid. ¹H NMR (500 MHz, CDCl₃): δ 8.74 (s, 1H), 7.76 (m, 6H), 7.64 (m, 3H), 7.55 (m, 6H), 7.06 (s, 2H), 6.41 (s, 1H), 3.85 (m, 8H), 2.85 (t, J = 6.7, 2H), 2.15 (m, 2H), 1.61 (m, 2H). ¹³C NMR: (125 MHz, CDCl₃): δ 160.6, 148.3, 139.3, 134.9, 133.8, 133.7, 130.4, 130.3, 121.3, 118.7, 118.0, 117.6, 101.7, 97.5, 56.1, 28.8, 28.6, 24.5, 22.5, 22.1, 21.4, 21.3. High resolution ESI-MS: m/z calculated for $C_{32}H_{33}N_3O_2P$ ([M+H]⁺): 522.2310; found 522.2297.

Synthesis of Amino functionalized PEG (6)

BochN
$$1. EDC, HOBt, DIPEA, R.T.$$
 H_3N TFA 6

In a 20 mL vial, 2.0 g (2.0 mmol) of MePEG₁₀₀₀-COOH (the PEG compound has on average 1000 Da molecular weight and 22 repeating units) was stirred with 575 mg (3.0 mmol) of EDC-HCl, 1 mL (5.7 mmol) of DIPEA and 270 mg (2.0 mmol) of HOBt in 10 mL of DCM for 30 min. To the mixture was added 544 mg (2.0 mmol) of *tert*-butyl(10-aminodecyl)carbamate (5, prepared using the reported procedure³) in 1 mL of MeOH and the mixture was stirred at room temperature for 16 h. The mixture was washed with 20 mL of water twice, and the organic layer was dried over Na₂SO₄ and filtered. The solution was concentrated using a rotary evaporator and purified by column chromatography on silica (flash gel) with a solvent gradient from DCM to 10:90 (v/v) MeOH-DCM. The resulting viscous liquid was stirred in 10 mL of TFA at room temperature for 12 h to deprotect the NH₂ group. The solution was concentrated using a rotary evaporator and precipitated in 40 mL of the 1:1 (v/v) mixture of hexane and ether. The resulting gel-like solid was dried under high vacuum to afford 480 mg (20%) of 8 as a waxy solid. ¹H NMR: δ 7.31 (m, 4H), 4.00 (s, 2H), 3.65 (m, 102H), 3.38 (s, 3H), 3.27 (m, 2H), 2.90 (m, 2H), 1.62 (m, 2H), 1.52 (m, 2H), 1.30 (m, 12H).

Polymer and Nanoparticle Synthesis

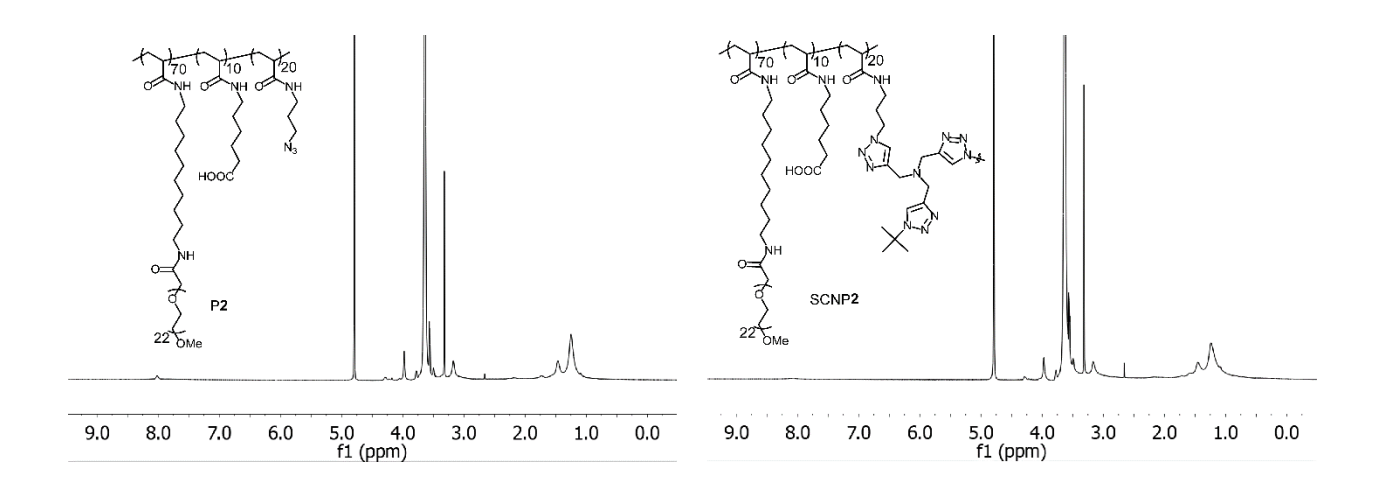
SCNP1 was prepared using the reported procedure.³

Synthesis of SCNP2

In a 20 mL screw-cap glass vial, 100 mg (4.1 μmol) of P1, 347 mg (289 μmol, 0.7 eq) of 6 and 5.4 mg (41 μmol, 0.1 eq) of 6-aminohexanoic acid were dissolved in a mixture of 1 mL of DMF and 100 μL of DIPEA. The vial was capped, sealed with parafilm, and stirred at 50 °C for 3 h. To the mixture, 17 mg (165 μmol, 0.4 eq) of 3-azidopropan-1-amine was added and stirred at 50 °C for another 3 h. The mixture was cooled to room temperature and precipitated in 14 mL of ethyl ether in a 15 mL centrifuge tube. P2 was collected by centrifugation and the supernatant was discarded. The gel-like solid was redissolved in 1 mL of MeOH in the centrifuge tube and 14 mL of ethyl ether was added to precipitate P2. The precipitate was collected by centrifugation, and supernatant was discarded. This process was repeated twice. The resulting gel-like polymer was dissolved in 3 mL of water and purified by dialysis (1 kD cut-off) with water for 16 h. The resulting solution was lyophilized to afford P2 as a gel-like solid.

In a 300 mL round bottom flask, 280 mg (3.0 μ mol) of P2 and 300 μ L of 100 mM DMSO solution of 7 were dissolved in 60 mL of water. To the mixture, 60 μ L of 100 mM aqueous solution of CuSO₄ and 20 mg of sodium ascorbate were added under N₂ atmosphere. The mixture was stirred at 30 °C for 2 h, and the temperature was raised to 50 °C and stirred overnight. Volatiles were removed using a rotary evaporator and resulting SCNP2 was dissolved in 3 mL of water. The SCNP2 solution was added with 1 g of Chelex 100 chelating resin, and the mixture was gently shaken overnight to remove copper ions. The resin was removed by filtration. The SCNP2 solution was purified by dialysis (1 kD cut-off) with 1 M aqueous solution of NaCl for 8 h and water for 48 h. The resulting solution was lyophilized to afford 251 mg (87%)

of SCNP2 as a white powder. The conversion of each step is almost quantitative, and the yield is typically range from 80-90% due to losses during the purification.



Synthesis of SCNP2-Cy5

In a 20 mL screw-cap glass vial, 46 mg (0.5 µmol) of P2 and 49 µL of 100 mM DMSO solution of 7 were dissolved in 10 mL of water and 25 µL of 10 mM DMSO solution of alkyne functionalized Cy5 was added. To the mixture were added 10 µL of 100 mM aqueous solution of CuSO₄ and 20 mg of sodium ascorbate under N₂ atmosphere. The mixture was stirred at 30 °C for 2 h, and the temperature was raised to 50 °C and stirred overnight. Volatiles were removed using a rotary evaporator and the resulting SCNP2-Cy5 was dissolved in 1 mL of water. The solution was added with 0.2 g of Chelex 100 chelating resin and the mixture was gently shaken overnight to remove copper ions. The resin was removed by filtration. The SCNP2-Cy5 solution was transferred to an Amicon tube with 10 kDa cut-off and washed 6 times with water.

Methods

Transmission electron microscopy (TEM)

To a UC-A on lacey gold TEM grid (Ted Pella) was added 8 μ L of 2 μ M solution of SCNP2 in fresh Milli-Q water. The SCNP solution was carefully removed after 20 min by using a filter paper to absorb the solution. Ammonium molybdate (2 wt% in water, 8 μ L) was added to the grid surface to negatively stain the SCNP. The staining process was conducted for 20 min and the solution was removed using a filter paper. The TEM grid was allowed to air dry for 1 h. The TEM imaging was performed on a JEOL 2100 Cryo TEM under 200 keV, and the images were processed using ImageJ.



Figure S1. TEM image of SCNP2.

Dynamic Light Scattering (DLS)

The SCNP solution was prepared in fresh Milli-Q water to a concentration of $20~\mu M$. To a disposable 4~mL plastic vial for the DLS instrument was added 1~mL of the solution and sonicated for around 30~s before the measurement. The light scattering and ζ -potential were subsequently measured by using a Marvin Instrument Ltd. nanoZS Zetasizer.

Saturation Transfer Difference (STD) experiment. BSA and Cu^{II} -SCNP2 were dissolved in deuterium oxide PBS buffer (1x, pD = 7.4) to reach the concentration of 100 μ M for both protein and nanoparticle. STD spectra were collected with the water suppression STD method on a VNS750 spectrometer with the bio-pack software. During the saturation period, the aromatic region on BSA protein was irradiated at 7 ppm, and the irradiation time was ranged from 0.5 s to 5 s. To minimize intramolecular signals from BSA, a 15 ms relaxation T_2 filter was applied during the data acquisition. Spectra were processed by MestReNova (v8.1), and STD effect intensity was calculated for the trimethyl ammonium peak at 3.0 ppm and alkyl chain peak at 1.2 ppm through the equation: STD = $(I_0 - I_{sat})/I_0$.

Fluorescence Polarization. Fluorescein labelled BSA protein was dissolved in PBS buffer (1x, pH = 7.4, with/without additional NaCl) at the concentration of 2 μ M with the concentration of Cu^{II}-SCNP2 ranging from 0 to 100 μ M. The solutions were transferred to a black 384-well plate, and 50 μ L of the solution was added to each well. The fluorescence polarization of solutions in each well was measured on an Analyst HT plate reader with the setup on fluorescein. The data was processed and fit using OriginPro2019.

Protein-Ligand Binding Simulation. The protein crystal structure was downloaded from protein data bank (PDB, https://www.rcsb.org/structure/2AVI).⁸ The data file was imported into Molecular Operating Environment (MOE). The chemical structure the biotin ligand was modified into Al8 or Al9, and the energy was minimized by the MOE software. The structure of the complex was color for annotation.

Fluorogenic Reactions. The fluorogenic CuAAC click reactions were performed in a 0.7 mL fluorimeter cuvette. Cu^{II}-SCNP was dissolved in 0.5 mL of PBS buffer (1x, pH = 7.4) in the cuvette. DMSO stock solutions of substrates and aqueous stock solutions of NaAsc were added to give a final concentration of $[NaAsc] = 200 \,\mu\text{M}$ and 2% (v/v) of DMSO. The click reaction of 3-azido-7-hydroxy-coumarin (Az1) or 7-ethynylcoumarin (Al11) restores its fluorescence. The intensity was monitored using a fluorimeter in kinetics mode, measuring the fluorescence intensity every 10 s at $\lambda_{em} = 480$ nm with excitation at $\lambda_{ex} = 410$ nm for Az1 and $\lambda_{em} = 420$ nm with excitation at $\lambda_{ex} = 328$ nm for Al11. The initial rate was determined using the following procedure: 30 s after the start of the reaction, where the fluorescence signals start to increase linearly over time, the slope of this linear part (around 10 data points) was calculated in counts per second (CPS) increase per minute. For the reaction between Az1 and Al1, the slope was calculated into the initial reaction rate in "µM/min" from the observed fluorescence intensity using the pure product as the standard. The initial reaction rates for the other alkyne substrates were calculated based on the assumption that the reactions reached 100% conversion, and the plateaued fluorescent signal was used as the fluorescence of the product. The fluorogenic CuAAC click reactions on BSA-Al were performed using a similar procedure with the initial rate presented directly as "CPS/min". The fluorogenic CuAAC click reactions on protein binder (Al1-10) were performed under the same procedure except the protein binder was premixed with the corresponding protein for 10 min before the start of the reaction.

For selective catalysis over BSA-Al and Al1. The fluorogenic CuAAC click reactions were performed in a 0.7 mL fluorimeter cuvette. In the total volume of 0.5 mL of PBS buffer (1x, pH = 7.4) containing Cu^{II}-SCNP1/Cu^{II}-SCNP2 (4 μ M) and BSA-Al (2 μ M) in the cuvette, DMSO stock solutions of Az1 and Al1 were added to give a final concentration of 40 μ M and 2% (v/v) of DMSO. NaAsc(aq) stock solution was added to give the final concentration of 200 μ M. The click reactions were performed for 20 min, and the solution was transferred to Amicon tubes with 10 kDa cutoff. The reaction mixture was washed with PBS buffer containing 10% DMSO for 6 times. The solutions passed through the tube were combined and the volume was normalized to 3 mL. The volume of the solution stayed in the tube was normalized to 3 mL. The solutions were measure by using a fluorimeter. λ_{em} = 430 -550 nm with excitation at λ_{ex} = 410 nm. The fluorescence intensity of the solution resided in the Amicon tube corresponded to the fluorogenic reaction on BSA-Al. The fluorescence intensity of the solution passed through the Amicon tube corresponded to the fluorogenic reaction on BSA-Al.

HPLC Yield Determination. The reaction was performed in a total volume of 2 mL of PBS buffer containing [Az1] = 20 μM, [Al1] = 40 μM, [Cu¹-SCNP2] = 2 μM and [NaAsc] = 200 μM at room temperature for 5 min. The mixture was extracted three times with 500 μL of DCM and separated by centrifugation. The organic layers were combined and evaporated under high vacuum. The resulting solid was redissolved in 400 μL of MeOH, and 100 μL of the solution was injected to a HPLC analysis for analysis. The HPLC standard curve was prepared by injecting the HPLC with 100 μL of 20, 100, 200 μM of synthetically prepared Al1-Az1 and detected with UV = 254 nm. The conversion was determined to be 105% by using the standard curve, which is within the error range (Figure S5).

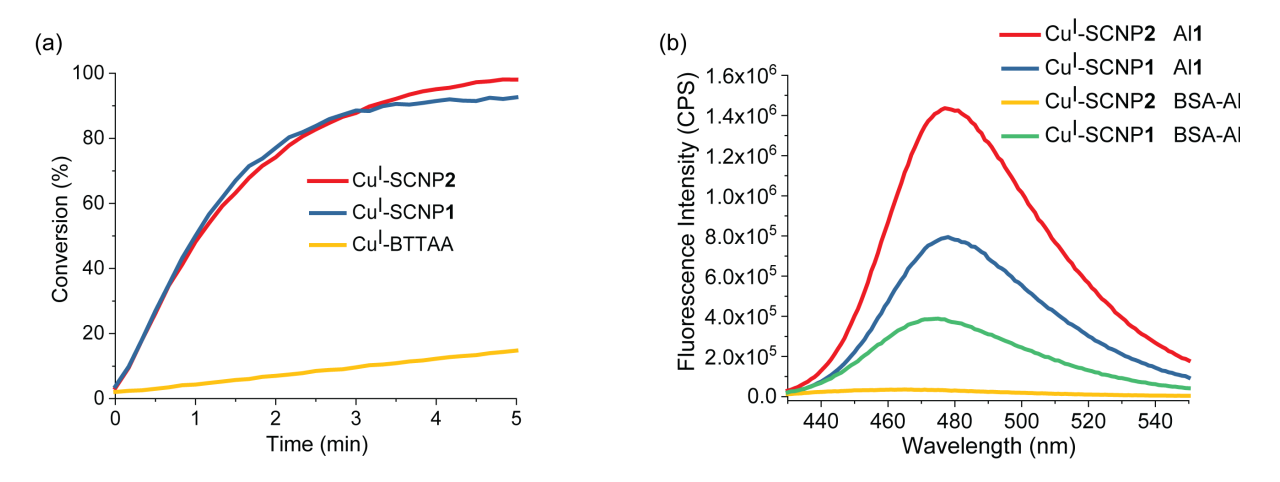


Figure S2. (a) Kinetics of reactions performed in PBS buffer containing [Az1] = $20 \,\mu\text{M}$, [Al1] = $40 \,\mu\text{M}$ and [NaAsc] = $200 \,\mu\text{M}$, by using [Cu^I-SCNP1] = $2 \,\mu\text{M}$, [Cu^I-SCNP2] = $2 \,\mu\text{M}$ or [Cu^I-BTTAA] = $20 \,\mu\text{M}$ as the catalyst. (b) Fluorescence spectra of the separated reaction mixtures in PBS buffer containing: [Cu^I-SCNP1/2] = $4 \,\mu\text{M}$, [Az1] = [Al1] = $40 \,\mu\text{M}$, [BSA-Al] = $2 \,\mu\text{M}$ and [NaAsc] = $200 \,\mu\text{M}$.

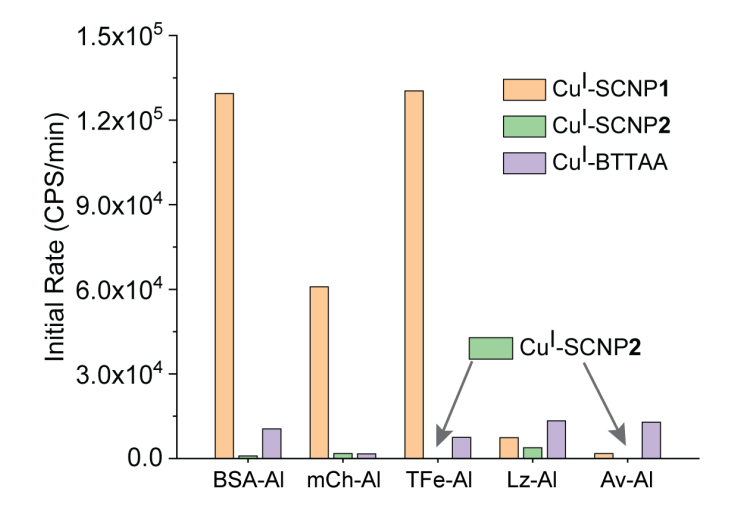


Figure S3. Initial reaction rates for small molecule and protein substrates with Cu^{II} –SCNP1 (2 μ M) or Cu^{II} –SCNP2 (2 μ M) in PBS buffer (1x, pH = 7.4) at room temperature. For protein substrate: protein (2 μ M, 5 μ M for Lz-Al) and Az1 (40 μ M). Data for SCNP1 and BTTAA from ref. 3.

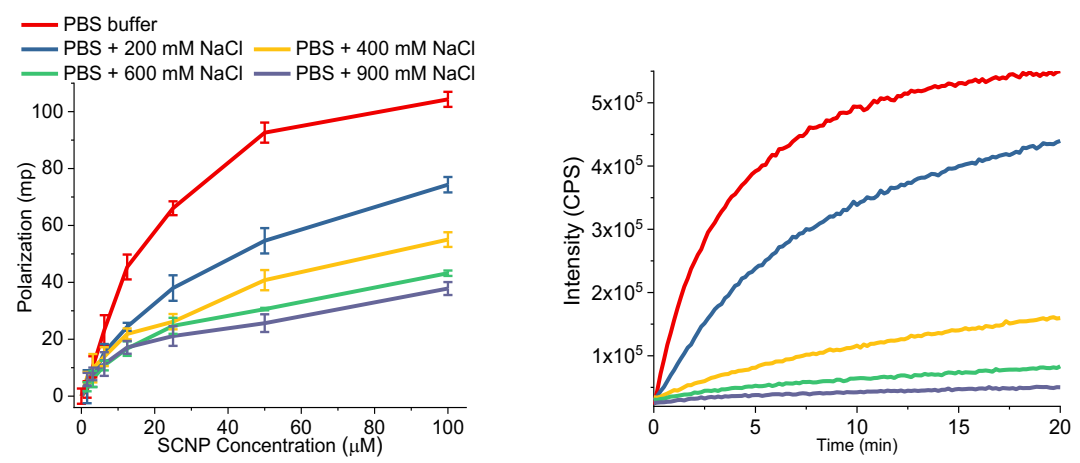


Figure S4. Fluorescence polarization of fluorescein labelled BSA (2 μ M) with different concentration of Cu^{II}–SCNP1 in PBS buffer (1x, pH = 7.4) with different amount of extra NaCl, and kinetics of reactions performed in PBS buffer containing [Az1] = 40 μ M, [BSA-Al] = 2 μ M and [NaAsc] = 200 μ M, by using [Cu^I-SCNP1] = 2 μ M as the catalyst in PBS buffer (1x, pH = 7.4) with different amount of extra NaCl,

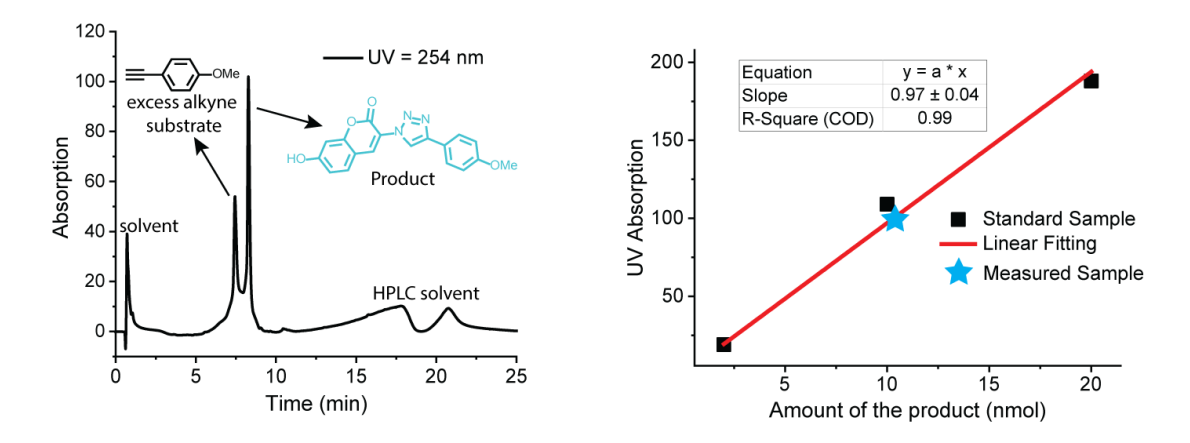


Figure S5. HPLC trace and the standard curve for the reaction conversion determination.

Cell Study

Cell Uptake of SCNPs. In Ibidi u-Dish 35 mm high dishes, 360000 HeLa cells in 3 mL of DMEM media (10% FBS added) containing Cu^{II}-SCNP1-Cy5 or Cu^{II}-SCNP2-Cy5 was added to each dish, and the cells were incubated at 37 °C with 5% CO₂ for 24 h. The cell media were removed, and each well was washed three times with 3 mL of PBS buffer. The images were taken by using confocal microscopy. Ex: 633 nm, em: 650-700 nm. (Figure S6)

Cell Uptake of Cu^I-SCNP2 Synthesized Compound. In Ibidi u-Dish 35 mm high dishes, 360000 HeLa cells in 3 mL of DMEM media (10% FBS added) was added to each dish, and the cells were incubated at 37 °C with 5% CO₂ for 24 h. The cell media were removed, and each well was washed three times with 3 mL of PBS buffer. To each well was added 2 mL of PBS buffer containing [Cu^{II}-SCNP2] = 1 μ M, [Az1] = 20 μ M and [Al1] = 20 μ M. The cell image was focused and 20 μ L of PBS buffer containing [NaAsc] = 20 mM was added. The images were taken by using confocal microscopy every 30 s. ex 405 nm, em 430-480 nm. The intensity reached to maximum after around 10 min.

Cytotoxicity of Cu^I-SCNP2. In a 96 wells plate, 10000 HeLa cells were added to each well with 100 μ L of DMEM media (10% FBS), and the cells were incubated at 37 °C with 5% CO₂ for 24 h. The cell media were removed, and each well was washed 2 times with 100 μ L of PBS buffer. To each well was added 50 μ L of PBS buffer containing 1, 2, 4, 8 or 16 μ M of Cu^{II}-SCNP2 and 100 μ M of NaAsc, and the cells were incubated at 37 °C for 30 min. To each well was added 50 μ L of DMEM media (10% FBS), and the cells were incubated for 24 h. The cell viability was measured by using MTT assay (Figure S8).

96 Wells Plate Drug Screening. In a 96 wells plate, 10000 HeLa cells were added to each well with 100 μL of DMEM media (10% FBS), and the cells were incubated at 37 °C with 5% CO₂ for 24 h. The cell media were removed, and each well was washed 2 times with 100 μL of PBS buffer. To each well was added 50 μL of PBS buffer containing 2% (v/v) DMSO, 1 μM of Cu^{II}-SCNP**2**, 40 μM of alkyne and azide substrates and 100 μM of NaAsc, and the cells were incubated at 37 °C for 30 min. To each well was added 50 μL of DMEM media (10% FBS), and the cells were incubated for 24 h. The cell viability was measured by using MTT assay. The experiments were performed twice and the average cell viability was presented in Figure 7. The control experiment was conducted under the same condition but without adding NaAsc (Figure S9).

Cytotoxicity of Al3-Az3. In a 96 wells plate, 10000 HeLa cells were added to each well with 100 μ L of DMEM media (10% FBS), and the cells were incubated at 37 °C with 5% CO₂ for 24 h. The cell media were removed, and each well was added DMEM media (10% FBS) containing Al3-Az3 from 320 μ M with 2x dilution and 0.5 % v/v DMSO. The cells were incubated at 37 °C for 24 h. The cell viability was measured by using MTT assay (Figure S10).

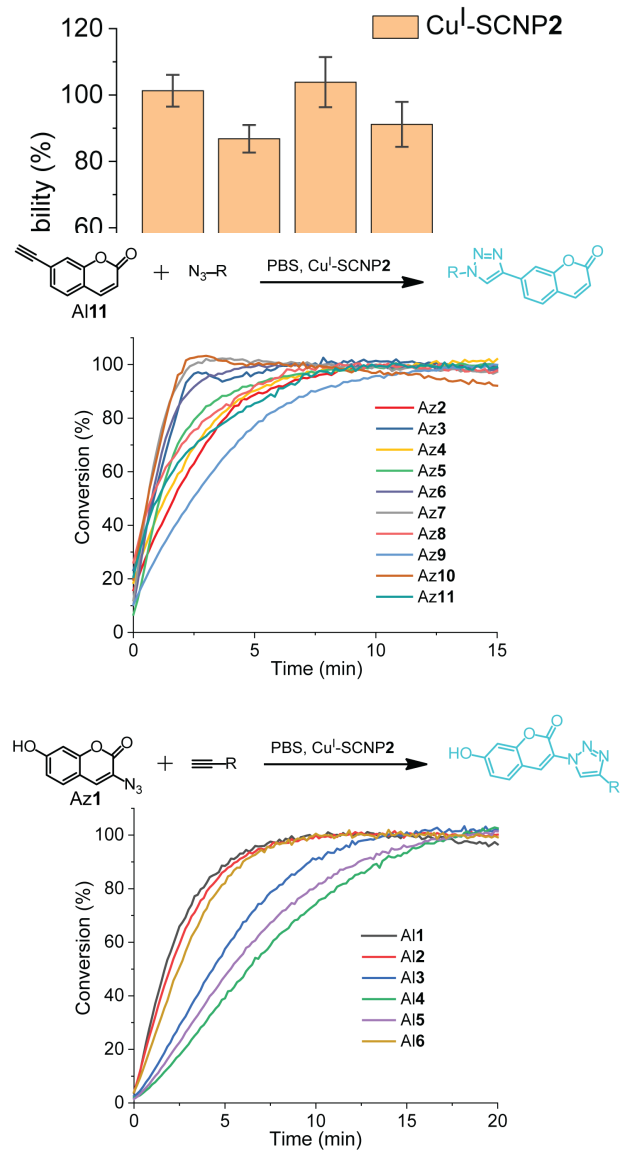


Figure S8. Fluorogenic reactions conducted with alkyne and azide substrates for drug screening. The reactions were performed in PBS buffer containing: $[Cu^I-SCNP2]=1~\mu M,~[Az]=[Al]=40~\mu M$ and $[NaAsc]=100~\mu M.$

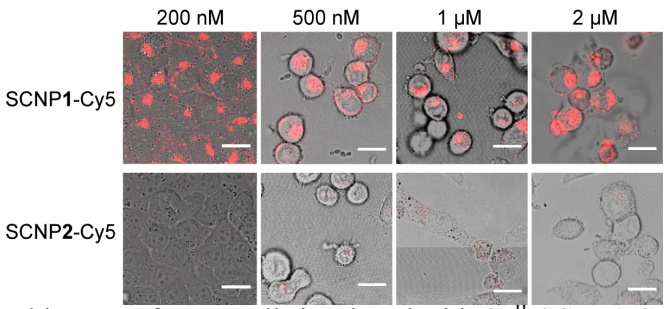


Figure S6. The confocal images of HeLa cells incubated with Cu^{II}-SCNP1-Cy5 or Cu^{II}-SCNP2-Cy5 for 24 h in DMEM media (10% FBS added).

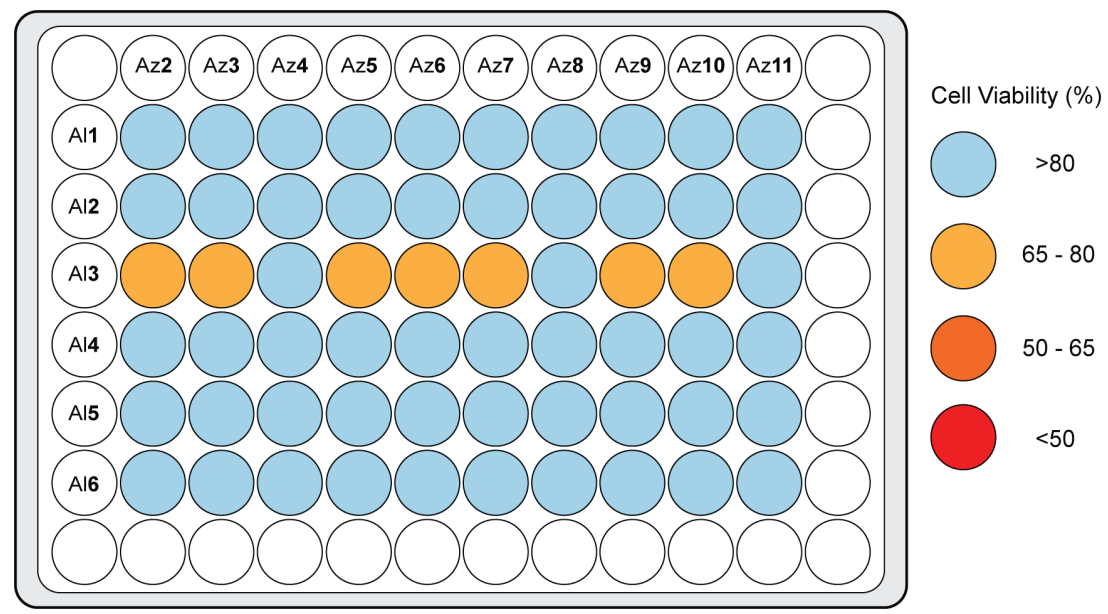


Figure S9. Control experiment performed for the 96 wells plate drug screening. The reactions were performed in PBS buffer containing: $[Cu^{I}-SCNP2] = 1 \mu M$, $[Az] = [Al] = 40 \mu M$ without NaAsc outside HeLa cells.

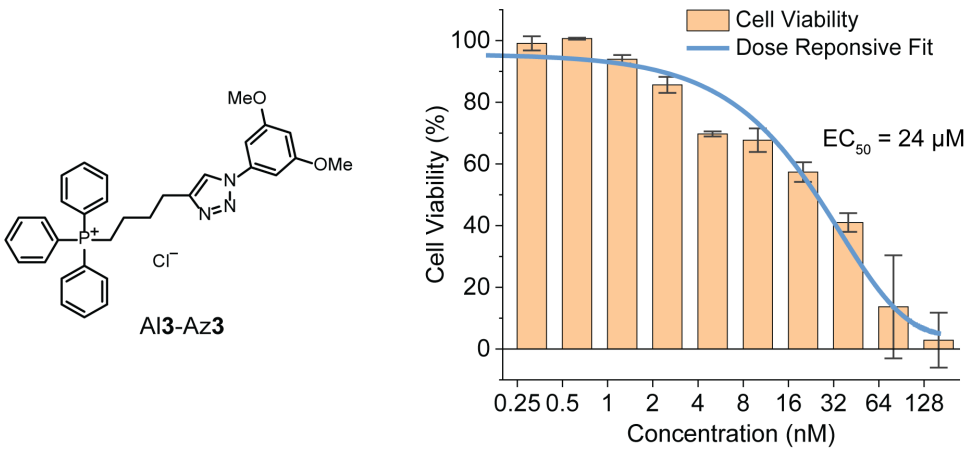


Figure S10. Cell viabilities of HeLa cells treated with different concentration of Al**3**-Az**3** in DMEM media (10% FBS).

Reference

- 1. Luo, J.; Theron, R.; Sewell, L. J.; Hooper, T. N.; Weller, A. S.; Oliver, A. G.; McIndoe, J. S. Rhodium-Catalyzed Selective Partial Hydrogenation of Alkynes. *Organometallics* **2015**, *34*, 3021-3028.
- 2. Chen, J.; Wang, J.; Bai, Y.; Li, K.; Garcia, E. S.; Ferguson, A. L.; Zimmerman, S. C. Enzyme-like Click Catalysis by a Copper-Containing Single-Chain Nanoparticle. *J. Am. Chem. Soc.* **2018**, *140*, 13695-13702.
- 3. Chen, J.; Wang, J.; Li, K.; Wang, Y.; Gruebele, M.; Ferguson, A. L.; Zimmerman, S. C. Polymeric "Clickase" Accelerates the Copper Click Reaction of Small Molecules, Proteins, and Cells. *J. Am. Chem. Soc.* **2019**, *141*, 9693-9700.
- Necardo, C.; Alfano, A. I.; Del Grosso, E.; Pelliccia, S.; Galli, U.; Novellino, E.; Meneghetti, F.; Giustiniano, M.; Tron, G. C. Aryl Azides as Forgotten Electrophiles in the Van Leusen Reaction: A Multicomponent Transformation Affording 4-Tosyl-1-arylimidazoles. J. Org. Chem. 2019, 84, 16299-16307.
- 5. Pagliai, F.; Pirali, T.; Del Grosso, E.; Di Brisco, R.; Tron, G. C.; Sorba, G.; Genazzani, A. A. Rapid Synthesis of Triazole-Modified Resveratrol Analogues via Click Chemistry. *J. Med. Chem.* **2006**, *49*, 467-470.
- 6. Bai, Y.; Feng, X.; Xing, H.; Xu, Y.; Kim, B. K.; Baig, N.; Zhou, T.; Gewirth, A. A.; Lu, Y.; Oldfield, E.; Zimmerman, S. C. A Highly Efficient Single-Chain Metal—Organic Nanoparticle Catalyst for Alkyne—Azide "Click" Reactions in Water and in Cells. *J. Am. Chem. Soc.* **2016**, *138*, 11077-11080.
- 7. Meng, G.; Guo, T.; Ma, T.; Zhang, J.; Shen, Y.; Sharpless, K. B.; Dong, J. Modular click chemistry libraries for functional screens using a diazotizing reagent. *Nature* **2019**, *574*, 86-89.
- 8. Livnah, O.; Bayer, E. A.; Wilchek, M.; Sussman, J. L. Three-dimensional structures of avidin and the avidin-biotin complex. *Proc. Natl. Acad. Sci* **1993**, *90*, 5076-5080.